



## A meshless technique based on the radial basis functions for solving systems of partial differential equations

Mehran Nemati, Mahmoud Shafiee\*, and Hamideh Ebrahimi

Department of Mathematics, Rasht Branch, Islamic Azad University, Rasht, Iran.

---

### Abstract

The radial basis functions (RBFs) methods were first developed by Kansa to approximate partial differential equations (PDEs). The RBFs method is being truly meshfree becomes quite appealing, owing to the presence of distance function, straight-forward implementation, and ease of programming in higher dimensions. Another considerable advantage is the presence of a tunable free shape parameter, contained in most of the RBFs that control the accuracy of the RBFs method. Here, the solution of the two-dimensional system of nonlinear partial differential equations is examined numerically by a Global Radial Basis Functions Collocation Method (GRBFCM). It can work on a set of random or uniform nodes with no need for element connectivity of input data. For the time-dependent partial differential equations, a system of ordinary differential equations (ODEs) is derived from this scheme. Like some other numerical methods, a comparison between numerical results with analytical solutions is implemented confirming the efficiency, accuracy, and simple performance of the suggested method.

---

**Keywords.** Global meshless method, Radial basis functions, Method of lines, Partial differential equations.

**2010 Mathematics Subject Classification.** 65L05, 34K06, 34K28.

### 1. INTRODUCTION

Meshfree methods do not need mesh generation, contrary to those of traditional numerical schemes used for solving partial differential equations [8]. The radial basis functions collocation methods are simple in programming. They are useful for a wide range of partial differential equations, especially for high-dimensional problems. It can be said that usage of kernels as trial functions, collocation in the symmetric and unsymmetric form first appeared in [22, 23]. It has been proved that this process is highly successful since the linear systems are generated easily along with proper accuracy and less computational expense. Furthermore, recently in [33] the optimality of the symmetric collocation [14, 20] which applies the kernel basis was proved in comparison with all existing linear PDE solvers which implement the same input data. The usage of RBFs for achieving the numerical solution of PDEs has been popular in science and engineering because it's a meshfree scheme and it can also be applied for multi-dimensional problems without difficulty. Many researchers have broadly used RBFs in various contexts including [7, 10, 14, 29] in recent years, and considered RBFs as a potential substitute in the area of numerical solution of PDEs. Hardy proposed RBFs interpolation in [16] for approximating two-dimensional geographical surfaces based on scattered data.

Kansa [24] applied a meshfree scheme based on multi-quadrics RBFs for approximating the solution of PDEs and then Golberg et. al extended this idea in [15]. The existence, uniqueness, and convergence of the approximation by RBFs was discussed in [20, 25, 27]. Huang et al. have discussed the significance of the role of shape parameter  $c$  in the MQ method in [21].

The solvability of the system of equations derived from this scheme for distinct points of interpolation has been presented in [27]. Very recently, in [1-4, 7, 28, 31, 35], the Local and Global Radial Basis Collocation Methods have

---

Received: 14 June 2020 ; Accepted: 02 April 2021.

\* Corresponding author. Email: mahmoudshafiee@gmail.com.

been used to achieve the meshfree solution of the nonlinear coupled PDEs. Kernel-based collocation methods for time-dependent PDEs are based on a fixed spatial interpolation. However, as coefficients are time-dependent, a system of ordinary differential equations (ODEs) is obtained. This scheme is known as the method of lines, and it suggests acceptable agreement in terms of accuracy in a myriad of problems [13].

It is aimed to approximate function  $f : \mathbb{R}^d \rightarrow \mathbb{R}$  by implementing RBF where  $d$  is the dimension of the problem and  $f(X)$  is data given at points  $X \in \mathbb{R}^d$  (named the centers) by the following interpolant

$$I_N f(X) = \sum_{j=1}^N \lambda_j \varphi(r_j), \tag{1.1}$$

where  $N$  is the number of data points,  $r_j = \|X - X_j\|$ ,  $\varphi$  is a standard RBF,  $r \geq 0$  and  $(\lambda_1, \lambda_2, \dots, \lambda_N)$  are the unknown coefficients which must be determined such that  $I_N f(X_j) = f(X_j)$  for  $j = 1, \dots, N$ . The standard RBFs fall into two separate categories;

Class 1. Infinitely smooth RBFs. The basis functions of this category are infinitely differentiable and they are considerably dependent on the shape parameter  $c$  e.g. Hardy multiquadric (MQ,  $\phi(r) = \sqrt{(r^2 + c^2)}$ ), Gaussian (GA,  $\phi(r) = \exp(-c^2 r^2)$ ), inverse multiquadric (IMQ,  $(\phi(r) = \sqrt{r^2 + c^2})^{-1}$ ) and inverse quadric (IQ,  $\phi(r) = (r^2 + c^2)^{-1}$ ) [10, 13, 15, 16, 24].

Class 2. Infinitely smooth (except at centers) RBFs. These basis functions are not infinitely differentiable. The accuracy of the aforementioned basis functions, which are free of the shape parameter, is relatively smaller in comparison with the basis functions of Class 1. For example, thin plate spline ( $r^{2n} \log(r)$ ,  $n = 1, 2, 3, \dots$ ), cubic  $r^3$  and linear  $r$ , etc.

In this work, we examine the numerical solution of the two-dimensional system of nonlinear (PDEs) by a Global Radial Basis Functions Collocation Method (GRBFCM). Such systems appear in many fields of mathematics, physical sciences, and engineering [9]. Obtaining the exact solution of these types of equations are usually too difficult and even if an exact solution is derived, the relevant calculations might very complex. Lately, some strong techniques have been proposed, such as the Adomian decomposition method [12, 34], the variational iteration method [17], the homotopy perturbation method [18, 19], and the differential transform method [11]. The GRBFCM belongs to a class of truly meshless methods which eliminates the need of underlying mesh. It works on a set of uniform or random nodes with no need for element connectivity of input data.

The rest of the paper is organized as follows. In section 2 we describe the governing equations and discuss the numerical method. Numerical experiments are given in section 3. A brief conclusion is presented in the last section.

## 2. MATHEMATICAL FORMULATION

In this section, the focus is on the numerical solution of the following two-dimensional system of nonlinear partial differential equations as the governing equations which was previously considered in [6, 9, 26] as

$$\begin{cases} V_t(X, t) - W(X, t)V_x(X, t) - W_t(X, t)V_y(X, t) = F(X, t), \\ W_t(X, t) - V(X, t)W_x(X, t) - V_t(X, t)W_y(X, t) = G(X, t), \end{cases} \quad X \in \Omega \subset \mathbb{R}^2, \quad t \in (0, T), \tag{2.1}$$

subject to the initial conditions

$$V(X, 0) = V_0(X), \quad X \in \bar{\Omega}, \tag{2.2}$$

$$W(X, 0) = W_0(X), \quad X \in \bar{\Omega}, \tag{2.3}$$

and Dirichlet boundary conditions

$$(V(X, t), W(X, t)) = (f^D(X, t), g^D(X, t)), \quad X \in \Gamma_D \subseteq \Gamma, \quad t \in [0, T], \tag{2.4}$$

where  $X = (x, y)$  and  $F, G, V_0, W_0, f^D$  and  $g^D$  are known functions,  $\Omega \subset \mathbb{R}^2$  is the domain,  $\Gamma$  is the boundary of the domain  $\Omega$ ,  $V$  and  $W$  are unknown functions which must be determined. Nonlinear systems of partial differential equations with variable coefficients are often too complicated to be solved exactly and even if an exact solution is obtained, the required calculations may be too complicated. In the literature, many powerful methods have been



proposed for (2.1). Arbabi et al. [6], extended the Haar wavelets method to obtain semi-analytical solutions for the nonlinear system of partial differential equations (2.1). Biazar and Eslami [9] proposed a new homotopy perturbation method (NHPM) for solving system (2.1). Matinfar et al. [26] introduced a new homotopy analysis method for obtaining solutions of systems of partial differential equations (2.1).

In the following, we choose discretization points  $X_i$ ,  $1 \leq i \leq n$ , and then rearrange the points successively into points  $\{X_I \cup X_D\}$  where  $X_I = \{X_1, \dots, X_{ni}\}$  is introduced as the set of interior points,  $X_D = \{X_{ni+1}, \dots, X_n\}$  is considered as the set of boundary points, and the notation  $ni$  is the number of interior points. Therefore, the unknown functions  $V(X, t)$  and  $W(X, t)$  can be approximated as

$$V(X, t) = \sum_{j=1}^n \alpha_j(t) \phi_j(X), \quad X \in \bar{\Omega}, \quad (2.5)$$

$$W(X, t) = \sum_{j=1}^n \beta_j(t) \phi_j(X), \quad X \in \bar{\Omega}, \quad (2.6)$$

where  $\phi_j(X) = \phi(\|X - X_j\|)$ ,  $\phi$  can be one of the RBFs listed in Table 1. The  $c \in \mathbb{R}$  in Table 1 is the shape parameter. Then we have

TABLE 1. Global RBFs.

Name	$\phi(r)$	condition
Gaussian	$\exp(-c^2 r^2)$	
Multiquadric	$(c^2 + r^2)^{\beta/2}$	$\beta \in \mathbb{R}_{\neq 0} \setminus 2\mathbb{N}$
Matérn/Sobolev	$r^\nu K_\nu(r)$	$\nu > 0$
Powers	$r^\beta$	$0 < \beta \notin 2\mathbb{N}$
Thin-plate splines	$r^{2n} \ln(r)$	$n \in \mathbb{N}$

$$V = \Phi \alpha(t),$$

$$W = \Phi \beta(t),$$

which in turn gives

$$\alpha(t) = \Phi^{-1} V, \quad (2.7)$$

$$\beta(t) = \Phi^{-1} W, \quad (2.8)$$

where

$$V = (V(X_1, t), V(X_2, t), \dots, V(X_n, t))^T,$$

$$W = (W(X_1, t), W(X_2, t), \dots, W(X_n, t))^T,$$

$$\alpha = (\alpha_1(t), \alpha_2(t), \dots, \alpha_n(t))^T,$$

$$\beta = (\beta_1(t), \beta_2(t), \dots, \beta_n(t))^T,$$

$$\Phi = (\phi_j(X_i))_{1 \leq i, j \leq n}.$$



Consequently, it is possible to estimate the partial derivatives of the approximate solution and from interpolants (2.5) and (2.6) we have

$$\frac{\partial}{\partial \xi}(V(X, t)) = \sum_{j=1}^n \alpha_j(t) \frac{\partial}{\partial \xi}(\phi_j(X)),$$

$$\frac{\partial}{\partial \xi}(W(X, t)) = \sum_{j=1}^n \beta_j(t) \frac{\partial}{\partial \xi}(\phi_j(X)),$$

where  $X \in \bar{\Omega}$  and  $\xi = x, y$ . From the aforementioned relations we obtain

$$\frac{\partial}{\partial \xi}(V(X_i, t)) = \frac{\partial \Phi_i}{\partial \xi} \Phi^{-1} V,$$

$$\frac{\partial}{\partial \xi}(W(X_i, t)) = \frac{\partial \Phi_i}{\partial \xi} \Phi^{-1} W,$$
(2.9)

where

$$\frac{\partial \Phi_i}{\partial \xi} = \left( \frac{\partial}{\partial \xi} \phi_1(X_i), \frac{\partial}{\partial \xi} \phi_2(X_i), \dots, \frac{\partial}{\partial \xi} \phi_n(X_i) \right).$$

At this point, it is possible to write the PDE (2.1) at the interior points  $X_i, i = 1, \dots, ni$ , as follows:

$$V_t(X_i, t) - W(X_i, t) \left( \sum_{j=1}^n \alpha_j(t) \frac{\partial}{\partial x} \phi_j(X_i) \right) - W_t(X_i, t) \left( \sum_{j=1}^n \alpha_j(t) \frac{\partial}{\partial y} \phi_j(X_i) \right) = F(X_i, t),$$

$$W_t(X_i, t) - V(X_i, t) \left( \sum_{j=1}^n \beta_j(t) \frac{\partial}{\partial x} \phi_j(X_i) \right) - V_t(X_i, t) \left( \sum_{j=1}^n \beta_j(t) \frac{\partial}{\partial y} \phi_j(X_i) \right) = G(X_i, t).$$

By taking (2.9), for  $i = 1, \dots, ni$ , we have

$$V_t(X_i, t) - W(X_i, t) ((\Phi_i)_x * \Phi^{-1} * V) - W_t(X_i, t) ((\Phi_i)_y * \Phi^{-1} * V) = F(X_i, t),$$

$$W_t(X_i, t) - V(X_i, t) ((\Phi_i)_x * \Phi^{-1} * W) - V_t(X_i, t) ((\Phi_i)_y * \Phi^{-1} * W) = G(X_i, t).$$
(2.10)

Matrix form of Eq. (2.10) is suggested in the following:

$$\tilde{V}_t - \tilde{W}_t * (\Phi_y \Phi^{-1} V) = \tilde{W} * (\Phi_x \Phi^{-1} V) + F,$$

$$\tilde{W}_t - \tilde{V}_t * (\Phi_y \Phi^{-1} W) = \tilde{V} * (\Phi_x \Phi^{-1} W) + G,$$
(2.11)

where

$$V = (V(X_1, t), \dots, V(X_n, t))^T,$$

$$W = (W(X_1, t), \dots, W(X_n, t))^T,$$

$$\tilde{V} = (V(X_1, t), \dots, V(X_{ni}, t))^T,$$

$$\tilde{W} = (W(X_1, t), \dots, W(X_{ni}, t))^T,$$

$$\Phi_x = ((\Phi_1)_x, \dots, (\Phi_{ni})_x)^T,$$

$$\Phi_y = ((\Phi_1)_y, \dots, (\Phi_{ni})_y)^T,$$

$$F = (F(X_1, t), \dots, F(X_{ni}, t))^T,$$

$$G = (G(X_1, t), \dots, G(X_{ni}, t))^T,$$



and  $*$  is a symbol referring to the pointwise product between two matrices or vectors.

The Dirichlet boundary condition which was appeared in (2.4), results in:

$$\begin{aligned} V(X_i, t) &= f^D(X_i, t), & i &= ni + 1, \dots, n, \\ W(X_i, t) &= g^D(X_i, t), & i &= ni + 1, \dots, n. \end{aligned} \quad (2.12)$$

By substituting (2.12) in (2.11) The system of ODEs is obtained with the following initial conditions:

$$\tilde{V}(0) = (V_0(X_i), i = 1, \dots, ni),$$

$$\tilde{W}(0) = (W_0(X_i), i = 1, \dots, ni).$$

It should be noted that the system of ODEs (2.11) is nonlinear, and an appropriate ODE solver in mathematical softwares will utilize a proper time-stepping automatically and recognize stiffness of the ODE system.

The following algorithm is considered as a summary for the above-mentioned section.

#### Algorithm

- 1: Select  $n$  discretization points in the domain  $\bar{\Omega}$ .
- 2: Rearrange discretization points into two sets of interior points and boundary points.
- 3: Form matrix  $\Phi$ .
- 4: Form matrix  $\Phi_x$ .
- 5: Form matrix  $\Phi_y$ .
- 6: Put vector  $F = (F(X_1, t), \dots, F(X_{ni}, t))^T$ .
- 7: Put vector  $G = (G(X_1, t), \dots, G(X_{ni}, t))^T$ .
- 8: Put initial vectors  $\tilde{V}(0) = (V_0(X_i))_{1 \leq i \leq ni}$  and  $\tilde{W}(0) = (W_0(X_i))_{1 \leq i \leq ni}$ .
- 9: Solve the system of ODEs

$$\tilde{V}_t - \tilde{W}_t * (\Phi_y * \Phi^{-1} * V) = \tilde{W} * (\Phi_x * \Phi^{-1} * V) + F,$$

$$\tilde{W}_t - \tilde{V}_t * (\Phi_y * \Phi^{-1} * W) = \tilde{V} * (\Phi_x * \Phi^{-1} * W) + G,$$

$$\text{where } V = \left( \tilde{V}, (f^D(X_i, t))_{ni+1 \leq i \leq n} \right)^T \text{ and } W = \left( \tilde{W}, (g^D(X_i, t))_{ni+1 \leq i \leq n} \right)^T.$$

### 3. NUMERICAL RESULTS

In this section, the numerical solution of the equations (2.1) with the right-hand side functions

$$F(X, t) = 1 - x + y + t,$$

$$G(X, t) = 1 - x - y - t,$$

initial conditions

$$V(X, 0) = x + y - 1,$$

$$W(X, 0) = x - y + 1,$$

and Dirichlet boundary conditions

$$V(0, y, t) = y + t - 1,$$

$$W(0, y, t) = -y - t + 1,$$

$$V(x, 0, t) = x + t - 1,$$

$$W(x, 0, t) = x - t + 1.$$

are presented. The exact solution of this problem is

$$V(X, t) = x + y + t - 1,$$

$$W(X, t) = x - y - t + 1.$$

We consider  $0 \leq x \leq 1$ ,  $0 \leq y \leq 1$  and  $t \geq 0$ . Three types of discretization points  $\{(x_i, x_j)\}_{1 \leq i, j \leq m}$  have been applied in the implementation of the method, which are listed as follows.



- Uniform points:

$$x_i = \frac{(i - 1)}{m - 1}, \quad i = 1, \dots, m.$$

- Legendre-Gauss-Lobatto points:

Let  $L_{m-1}$  be the Legendre polynomial of degree  $m - 1$ . The  $x_i, i = 1, \dots, m$  are the zeros of  $(1 - x^2)L'_{m-1}(x)$ . Then  $x_i, i = 1, \dots, m$  belong to the interval  $[-1, 1]$  and can be easily transferred to the interval  $[0, 1]$  by the transformation  $y = \frac{1}{2}(x + 1)$ .

- Chebyshev-Gauss-Lobatto points:

$$x_i = -\cos\left(\frac{\pi(i - 1)}{m - 1}\right), \quad i = 1, \dots, m,$$

which is in the interval  $[-1, 1]$  and can be effortlessly transferred to the interval  $[0, 1]$  by the transformation  $y = \frac{1}{2}(1 + x)$ .

Here, the Powers ( $\beta = 5$ ), Matérn ( $\nu = 1$ ), Multiquadric ( $\beta = 1$ ) and Thin-plate splines ( $n = 3$ ) RBFs are applied. In order to have a well-conditioned system matrix, the shape parameter  $c$  should not be very large. Although in order to get proper accuracy by the RBF method large shape parameters are needed, this leads to the ill-conditioned system matrix. Thus, it is obvious that having the best accuracy and conditioning can not occur simultaneously. This fact is considered as the Uncertainty Principle, which shows the more desired value of one quantity is the less desired value of the other is [32].

The shape parameter  $c$  can be selected so that the collocation matrix  $\Phi$  has a condition number,  $\kappa(\Phi)$ , in the range  $10^{13} \leq \kappa(\Phi) \leq 10^{15}$  [31]. These limits for the condition number are reliable until computers that perform double-precision floating-point arithmetic are utilized, but they will differ when applying other floating-point number systems [30]. The selection of the shape parameter at each center is explained in the following pseudocode [31]:

```

kappa = 0
while kappa < kappaMin and kappa > kappaMax do
  form  $\Phi$ 
   $[V, S, W] = \text{svd}(\Phi)$ 
   $\text{kappa} = \frac{\max(S)}{\min(S)}$ 
  if kappa < kappaMin then
    shape = shape - shapeIncrement
  else if kappa > kappaMax then
    shape = shape + shapeIncrement
  end if
end while

```

The ODE solver ode23t of MATLAB is applied to the last ODE system (2.11). The maximum absolute and root mean squared error norms are considered as follows.

$$L_2 = \sqrt{\frac{1}{n} \sum_{j=1}^n |V_j - \bar{V}_j|^2},$$

$$L_\infty = \max_{1 \leq j \leq n} |V_j - \bar{V}_j|,$$



where  $V$  and  $\bar{V}$  are the exact and approximate solutions, respectively. The  $L_2$  error norms using the proposed method with various numbers and kinds of points including Chebyshev, Legendre, and uniform points and with different RBFs including Powers ( $\beta = 5$ ), Matérn ( $\nu = 1$ ), Multiquadric ( $\beta = 1$ ) and Thin-plate splines ( $n = 3$ ) at time  $T = 0.01$  are reported in Tables 2-5. Tables 2-5 show that by the present method, a bit more accurate solutions are obtained for Chebyshev points. Also for all the tested RBFs, the Powers RBF yield a little more accurate results. In Tables 6 and 7, implementation of the method with  $n = 81$  uniform points and different RBFs are shown against some other methods [6, 9, 26] at selected points. Tables 6 and 7 show that the results of the presented method are quite accurate and stable. Distributions of absolute error with their contours at  $T = 0.01$  for  $n = 100$  uniform points with various RBFs including Powers ( $\beta = 5$ ), Matérn ( $\nu = 1$ ), Multiquadric ( $\beta = 1$ ) and Thin-plate splines ( $n = 3$ ) are shown in Figures 1-4.

TABLE 2. The  $L_2$  error norms of  $V$  and  $W$  at time  $T = 0.01$  with various numbers and kinds of points and with Powers RBF.

$n$	V			W		
	Uniform points	Legendre points	Chebyshev points	Uniform points	Legendre points	Chebyshev points
36	$3.49E - 04$	$1.41E - 04$	$1.07E - 04$	$3.58E - 04$	$1.39E - 04$	$1.45E - 04$
64	$1.02E - 04$	$2.90E - 05$	$2.14E - 05$	$1.02E - 04$	$2.83E - 05$	$2.08E - 05$
100	$4.48E - 05$	$9.97E - 06$	$6.79E - 06$	$4.45E - 05$	$9.87E - 06$	$6.75E - 06$
144	$2.37E - 05$	$8.91E - 06$	$2.75E - 06$	$2.35E - 05$	$8.84E - 06$	$2.84E - 06$

TABLE 3. The  $L_2$  error norms of  $V$  and  $W$  at time  $T = 0.01$  with various numbers and kinds of points and with Matérn RBF.

$n$	V			W		
	Uniform points	Legendre points	Chebyshev points	Uniform points	Legendre points	Chebyshev points
36	$2.33E - 04$	$1.70E - 04$	$1.51E - 04$	$8.93E - 05$	$7.23E - 05$	$6.64E - 05$
64	$1.55E - 04$	$9.43E - 05$	$8.13E - 05$	$6.28E - 05$	$4.44E - 05$	$3.99E - 05$
100	$1.12E - 04$	$5.96E - 05$	$5.07E - 05$	$4.75E - 05$	$3.06E - 05$	$2.76E - 05$
144	$8.68E - 05$	$4.11E - 05$	$3.48E - 05$	$3.78E - 05$	$2.30E - 05$	$2.10E - 05$

TABLE 4. The  $L_2$  error norms of  $V$  and  $W$  at time  $T = 0.01$  with various numbers and kinds of points and with Multiquadric RBF.

$n$	V			W		
	Uniform points	Legendre points	Chebyshev points	Uniform points	Legendre points	Chebyshev points
36	$1.15E - 03$	$8.48E - 04$	$7.42E - 04$	$8.58E - 04$	$6.30E - 04$	$5.55E - 04$
64	$7.70E - 04$	$4.13E - 04$	$3.34E - 04$	$5.48E - 04$	$3.10E - 04$	$2.58E - 04$
100	$5.36E - 04$	$2.07E - 04$	$1.64E - 04$	$3.76E - 04$	$1.63E - 04$	$1.32E - 04$
144	$3.84E - 04$	$1.08E - 04$	$8.72E - 05$	$2.69E - 04$	$8.81E - 05$	$7.04E - 05$



TABLE 5. The  $L_2$  error norms of  $V$  and  $W$  at time  $T = 0.01$  with various numbers and kinds of points and with Thin-plate splines RBF.

$n$	V			W		
	Uniform points	Legendre points	Chebyshev points	Uniform points	Legendre points	Chebyshev points
36	$1.09E - 04$	$1.19E - 04$	$8.88E - 05$	$1.04E - 04$	$1.15E - 04$	$8.36E - 05$
64	$9.62E - 05$	$7.01E - 05$	$6.36E - 05$	$9.24E - 05$	$6.77E - 05$	$6.11E - 05$
100	$7.60E - 05$	$4.42E - 05$	$3.78E - 05$	$7.37E - 05$	$4.33E - 05$	$3.71E - 05$
144	$6.19E - 05$	$3.06E - 05$	$2.56E - 05$	$6.04E - 05$	$3.03E - 05$	$2.56E - 05$

TABLE 6. Results for  $V$  at time  $T = 0.01$ , with  $n = 81$  uniform points.

$(x, y)$	(0.125, 0.125)	(0.125, 0.625)	(0.375, 0.375)	(0.375, 0.875)	(0.625, 0.125)	(0.875, 0.875)
Exact	-0.74	-0.24	-0.24	0.26	-0.24	0.76
Matérn RBF	-0.740054	-0.239999	-0.240001	0.259932	-0.240069	0.759989
Power RBF	-0.740014	-0.240002	-0.240001	0.259996	-0.240008	0.759992
Multiquadric RBF	-0.740178	-0.240072	-0.240012	0.259603	-0.240183	0.759673
Thin-plate splines RBF	-0.740007	-0.239985	-0.240004	0.260042	-0.240082	0.759977
Ref. [6]	-0.739849	-0.239854	-0.239528	0.260446	-0.239391	0.760789
Ref. [9]	-0.730000	-0.230000	-0.230000	0.269999	-0.230000	0.769999
Ref. [26]	-0.730000	-0.230000	-0.230000	0.269999	-0.230000	0.769999

TABLE 7. Results for  $W$  at  $T = 0.01$ , with  $n = 81$  uniform points.

$(x, y)$	(0.125, 0.125)	(0.125, 0.625)	(0.375, 0.375)	(0.375, 0.875)	(0.625, 0.125)	(0.875, 0.875)
Exact	-0.749	-0.249	-0.249	0.251	-0.249	0.751
Matérn RBF	-0.749005	-0.248999	-0.249000	0.250993	-0.249006	0.750999
Power RBF	-0.749001	-0.249000	-0.249000	0.250999	-0.249000	0.750999
Multiquadric RBF	-0.749016	-0.249007	-0.249001	0.250996	-0.249017	0.750969
Thin-plate splines RBF	-0.749007	-0.248998	-0.249000	0.251004	-0.249008	0.750997
Ref. [6]	-0.748998	-0.248998	-0.248995	0.251003	-0.248993	0.751007
Ref. [9]	-0.748000	-0.248000	-0.248000	0.251999	-0.248000	0.751999
Ref. [26]	-0.748000	-0.248000	-0.248000	0.251999	-0.248000	0.751999





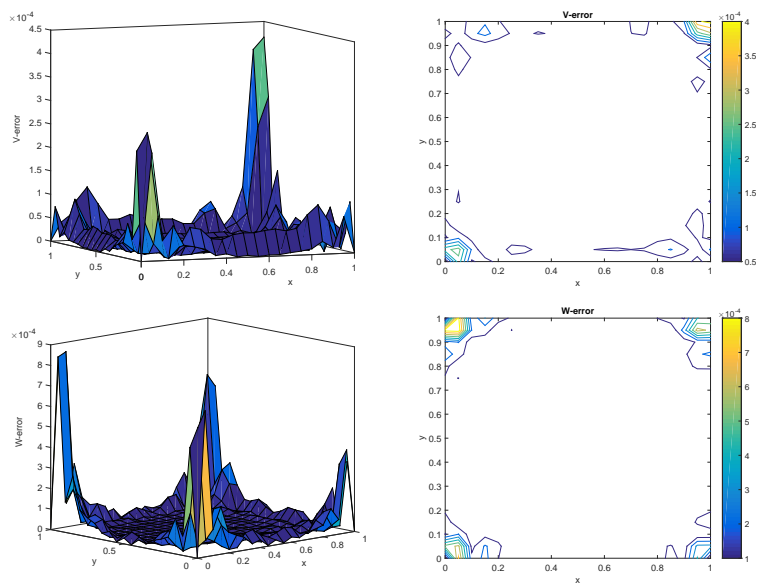


FIGURE 1. Graphs of absolute error with their contours at  $T = 0.01$  by Powers RBF and  $n = 100$  uniform points.

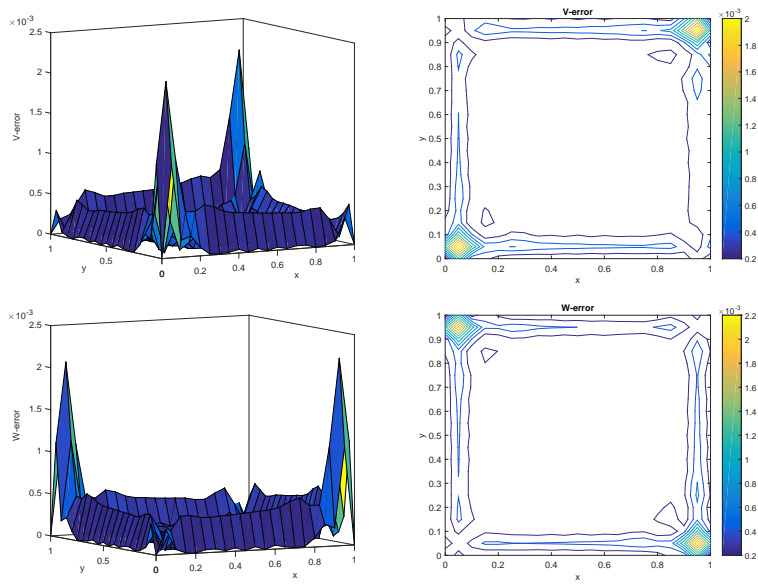


FIGURE 2. Graphs of absolute error with their contours at  $T = 0.01$  by Matérn RBF and  $n = 100$  uniform points.



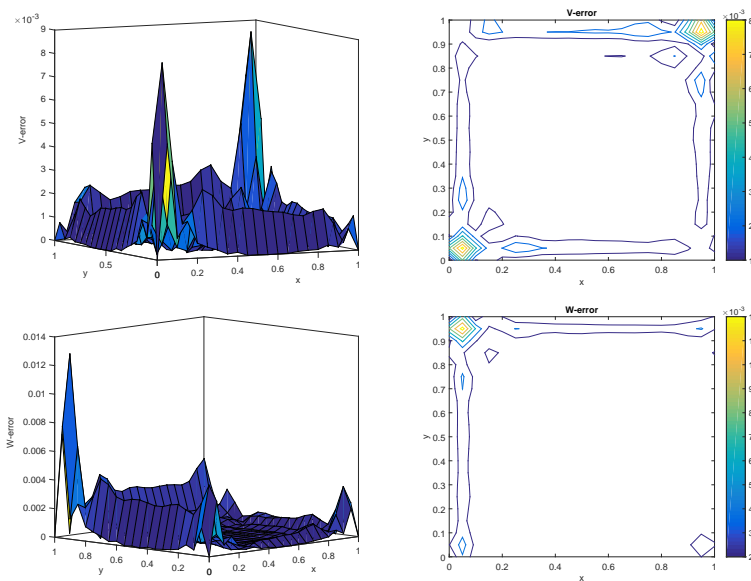


FIGURE 3. Graphs of absolute error and their contours at time  $T = 0.01$  by Multiquadric RBF and  $n = 100$  uniform points.

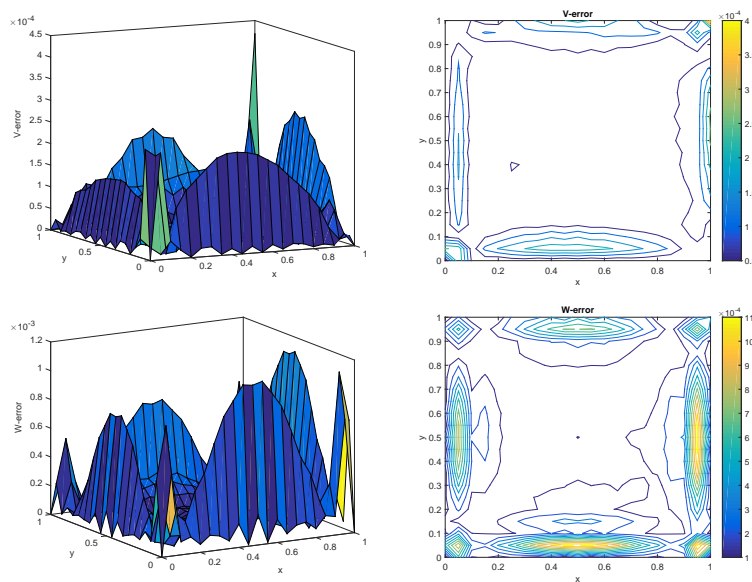


FIGURE 4. Graphs of absolute error and their contours at time  $T = 0.01$  by Thin-plate splines RBF and  $n = 100$  uniform points.



## 4. CONCLUSION

RBFs play an important role in solving PDEs as a meshfree scheme. The most important advantage of the RBFs method is the meshless property compared with the traditional mesh dependent techniques like finite element and finite difference schemes.

In this work, we extended the concept of efficient Global Radial Basis Functions Collocation Method which was presented in [6, 9, 26] for solving the two-dimensional system of nonlinear partial differential equations numerically which is applied to a set of uniform or random nodes with no need for element connectivity of input data. Obtained numerical results by the proposed method offer a very high accuracy in the computations. Also, using the method the cost of computations and discretization of variables reduced strongly.

## REFERENCES

- [1] M. Abbaszadeh and M. Dehghan, *Meshless upwind local radial basis function-finite difference technique to simulate the time-fractional distributed-order advection-diffusion equation*, Engineering with computers, (2019), 1–17.
- [2] M. Abbaszadeh and M. Dehghan, *Reduced order modeling of time-dependent incompressible Navier-Stokes equation with variable density based on a local radial basis functions-finite difference (LRBF-FD) technique and the POD/DEIM method*, Computer Methods in Applied Mechanics and Engineering, 364 (2020), 112914.
- [3] M. Abbaszadeh and M. Dehghan, *An upwind local radial basis functions-differential quadrature (RBFs-DQ) technique to simulate some models arising in water sciences*, Ocean Engineering, 197 (2020), 106844.
- [4] M. Abbaszadeh and M. Dehghan, *Simulation flows with multiple phases and components via the radial basis functions-finite difference (RBF-FD) procedure: Shan-Chen model*, Engineering Analysis with Boundary Elements, 119 (2020), 151–161.
- [5] A. Ali and S. Haq, *A computational meshfree technique for the numerical solution of the two-dimensional coupled Burgers' equations*, International Journal for Computational Methods in Engineering Science and Mechanics, 10(5) (2009), 406–422.
- [6] S. Arbabi, A. Nazari, and M. T. Darvishi, *A two-dimensional Haar wavelets method for solving systems of PDEs*, Applied Mathematics and Computation, 292 (2017), 33–46.
- [7] S. N. Atluri and S. Shen, *The Meshless Local Petrov-Galerkin (MLPG) method: A simple & less-costly alternative to the finite element and boundary element methods*, Computer Modeling in Engineering and Sciences, 3 (1) (2002), 11–51.
- [8] T. Belytschko, et al, *Meshless methods: an overview and recent developments*, Computer methods in applied mechanics and engineering, 139(1-4) (1996), 3–47.
- [9] J. Biazar and M. Eslami, *A new homotopy perturbation method for solving systems of partial differential equations*, Computers & Mathematics with Applications, 62(1) (2011), 225–234.
- [10] M. D. Buhmann, *Radial basis functions: theory and implementations*, Cambridge university press, 2003.
- [11] C. K. Chen and S. H. Ho, *Solving partial differential equations by two-dimensional differential transform method*, Applied Mathematics and computation, 106(2-3) (1999), 171–179.
- [12] Y. Cherruault and G. Adomian, *Decomposition methods: a new proof of convergence*, Mathematical and Computer Modelling, 18(12) (1993), 103–106.
- [13] Y. Dereli and R. Schaback, *The meshless kernel-based method of lines for solving the equal width equation*, Applied Mathematics and Computation, 219(10) (2013), 5224–5232.
- [14] G. E. Fasshauer, *Solving partial differential equations by collocation with radial basis functions*, Proceedings of Chamonix 1997, (1996), 1–8.
- [15] M. A. Golberg, C. S. Chen, and S. R. Karur, *Improved multiquadric approximation for partial differential equations*, Engineering Analysis with boundary elements 18(1) (1996), 9–17.
- [16] R. L. Hardy, *Multiquadric equations of topography and other irregular surfaces*, Journal of geophysical research, 76(8) (1971), 1905–1915.
- [17] J. H. He, *Variational iteration method—a kind of non-linear analytical technique: some examples*, International journal of non-linear mechanics, 34(4) (1999), 699–708.



- [18] J. H. He, *Homotopy perturbation technique*, Computer methods in applied mechanics and engineering, 178(3-4) (1999), 257–262.
- [19] J. H. He, *A coupling method of a homotopy technique and perturbation technique for non-linear problems*, International journal of non-linear mechanics, 35(1) (2000), 37–43.
- [20] C. Franke and R. Schaback, *Convergence order estimates of meshless collocation methods using radial basis functions*, Advances in computational mathematics, 8(4) (1998), 381–399.
- [21] C-S. Huang, C-F. Lee, and AH-D. Cheng, *Error estimate, optimal shape factor, and high precision computation of multiquadric collocation method*, Engineering Analysis with Boundary Elements, 31(7) (2007), 614–623.
- [22] C. Franke and R. Schaback, *Solving partial differential equations by collocation using radial basis functions*, Applied Mathematics and computation, 93(1) (1998), 73–82.
- [23] E. J. Kansa, *Application of Hardy's multiquadric interpolation to hydrodynamics*, (1986), 111–116.
- [24] E. J. Kansa, *Multiquadrics -A scattered data approximation scheme with applications to computational - I surface approximations and partial derivative estimates*, Computers & Mathematics with applications, 19(8-9) (1990), 127–145.
- [25] W. R. Madych and S. A. Nelson, *Multivariate interpolation and conditionally positive definite functions. II*, Mathematics of Computation, 54(189) (1990), 211–230.
- [26] M. Matinfar, M. Saeidy, and B. Gharahsuflu, *A new homotopy analysis method for finding the exact solution of systems of partial differential equations*, Selcuk university Research center of Applied Mathematics, 2012.
- [27] C. A. Micchelli, *Interpolation of scattered data: distance matrices and conditionally positive definite functions*, Constructive approximation, 2(1) (1986), 11–22.
- [28] M. Mohammadi, F. S. Zafarghandi, E. Babolian, and S. Jvadi, *A local reproducing kernel method accompanied by some different edge improvement techniques: application to the Burgers' equation*, Iranian Journal of Science and Technology, Transactions A: Science, 42(2) (2018), 857–871.
- [29] S. Müller and R. Schaback, *A Newton basis for kernel spaces*, Journal of Approximation theory, 161(2) (2009), 645–655.
- [30] M. L. Overton, *Numerical computing with IEEE floating point arithmetic*, Society for Industrial and Applied Mathematics, 2001.
- [31] S. A. Sarra, *A local radial basis function method for advection–diffusion–reaction equations on complexly shaped domains*, Applied mathematics and Computation, 218(19) (2012), 9853–9865.
- [32] R. Schaback, *Error estimates and condition numbers for radial basis function interpolation*, Advances in Computational Mathematics, 3(3) (1995), 251–264.
- [33] R. Schaback, *A computational tool for comparing all linear PDE solvers*, Advances in Computational Mathematics, 41(2) (2015), 333–355.
- [34] A. M. Wazwaz, *The decomposition method applied to systems of partial differential equations and to the reaction–diffusion Brusselator model*, Applied mathematics and computation, 110(2-3) (2000), 251–264.
- [35] F. S. Zafarghandi, et al, *A localized Newton basis functions meshless method for the numerical solution of the nonlinear coupled Burgers' equations*, International Journal of Numerical Methods for Heat & Fluid Flow, 2017.

